
Since January 2020 Elsevier has created a COVID-19 resource centre with free information in English and Mandarin on the novel coronavirus COVID-19. The COVID-19 resource centre is hosted on Elsevier Connect, the company's public news and information website.

Available online at www.sciencedirect.com
ScienceDirect
Journal of the Chinese Institute of Chemical Engineers 39 (2008) 187–193
JOURNAL OF THE CHINESE INSTITUTE OF CHEMICAL ENGINEERS
www.elsevier.com/locate/jcice

# Enhancement of target-DNA hybridization efficiency by pre-hybridization on sequence-orientated micro-arrayed probes

Dan-Kai Yang [a], Jie-Len Huang [b], Chia-Chun Chen [b], Hung-Ju Su [b,*], Jui-Chuang Wu [a,*]

[a] *R&D Center for Membrane Technology and Chemical Engineering Department, Chung Yuan Christian University, Chung Li, Tao Yuan 32023, Taiwan*
[b] *Biomedical Engineering Center, Industrial Technology Research Institute, Chu Tung, Hsin Chu 31040, Taiwan*

Received 12 June 2007; accepted 24 December 2007

**Abstract**

The enhancement of hybridization efficiency of deoxyribonucleic acid (DNA) targets using oligonucleotide pre-hybridization is studied on two sequence-inversed micro-arrayed probes. The sequences for pre-hybridizing both oligo and target DNA are designed to be fully complementary with their shared DNA probe in a coaxial stacking configuration; i.e. they hybridize immediately alongside each other along the continuous complement probe strand. The pre-hybridizing oligo and target DNA are differentiated by being labeled with two distinct fluorescent dyes, and the cooperative effect on hybridization efficiency is investigated through the comparison of the stacking and individual hybridization configurations based on the detection signals of the labeling dyes. The results show that the pre-hybridization of a DNA oligo enhances the subsequent hybridization efficiency of the target-DNA coupling onto the same probe. The efficiency is enhanced if the hybridization position occurs at a site close to the substrate surface.


*Keywords:* Hybridization efficiency; DNA micro-array; Molecular steric hindrance; DNA biochips; Pre-hybridization; DNA sequence orientation; DNA probes

## 1. Introduction

With the benefits inherited from the manufacturing process of the semiconductor industry and the completion of human gene decoding project in the 1980s and 1990s, deoxyribonucleic acid (DNA) biochip technology has progressed rapidly and has been widely applied in clinical diagnosis (Wang and Cheng, 2005), drug screening (Schaack *et al.*, 2005), agriculture (Douglas and Ehlting, 2005), and many other fields. Further development of this technology is still being undertaken, particularly in the area of improving the hybridization efficiency of immobilized DNA probes with their sample targets. The current research efforts are rooted in the understanding that the hybridization efficiency directly indicates the success of the experimental design and further data interpretation.

The hybridization efficiency of DNA chips is critically affected by the nucleotide structure of the probe and target (Koehler and Peyret, 2005), addition of a stabilizer (Maruyama *et al.*, 2001), probe immobilization (Zammatteo *et al.*, 2000), and also hybridization conditions such as incubation temperature and salt concentration (Rule *et al.*, 1997), electric field (Fixe *et al.*, 2004), agitation or mixing (Deng *et al.*, 2006; McQuain *et al.*, 2004), and substrate surface conditions (Guo *et al.*, 1994; Wu *et al.*, 2006). In addition to these overall conditions, the molecular-level approach has also been reported to improve the hybridization efficiency of micro-arrayed DNA. This approach builds on the theory that the DNA coupling efficiency is affected by the spatial molecular interaction (Wu and Prausnitz, 2002), so that the introduction of a spacer element in a probe is able to enhance the proceeding hybridization efficiency.

The steric effect on DNA hybridization efficiency in fact gives a broader consideration beyond the inter-molecular repulsion. It covers the effects resulting from the space and location occupied by DNA or other small molecules, and many research efforts have been devoted to this topic. Luo *et al.* (2002) introduced a spacer element and a minor groove binder molecule in a probe to enhance array hybridization efficiency. Ezaki *et al.* (2003) used p53 protein to promote spatial hybrid formation and identify mismatches. Tao *et al.* (2003) reported a

* Corresponding authors.
*E-mail addresses:* suhungju@itri.org.tw (H.-J. Su), ray_j_wu@cycu.edu.tw (J.-C. Wu).

0368-1653/$ – see front matter © 2008 Published by Elsevier B.V. on behalf of Taiwan Institute of Chemical Engineers.
doi:10.1016/j.jcice.2007.12.012

novel technique to block the non-target strand of the double-stranded DNA sample and improve the molecular interaction to gain the hybridization efficiency. Hong *et al.* (2005) recently presented a nano-size substrate surface to confine probes within a spatial region to control non-specific hybridization. All of these efforts have focused on using complicated molecule-level techniques to improve the hybridization efficiency. There is still a lack of direct evidence to reveal how the steric effect influences the hybridization efficiency of DNA micro-arrayed chips.

In this regard, this study reports an approach to directly uncover the hindrance effect on the hybridization efficiency of micro-arrayed DNA. We designed two probes with two reverse sequence blocks, so that two oligonucleotide targets hybridize onto their shared probes in a coaxial stacking configuration; i.e. two targets hybridize immediately next to each other along the continuous complement probe strand, as shown in Fig. 1. The steric effect is investigated through the comparison between the stacking and individual hybridization schemes based on the detection signals of the labeling dyes. Through this simple, yet unique experimental design, we demonstrate the cooperative molecular steric effect on the hybridization efficiency of single-stranded DNAs with their complementary immobilized probes on DNA chips.

## 2. Experimental

### 2.1. Materials and methods

#### 2.1.1. DNA probes and targets

The sequence of probe #1 is 5′-amine-$C_6$-(GTGATTGGTCGCGGTGA)-(CGCAAGTTAGGTTTTGTCAAGAAAGGGTGTAACGCAACTAAGTCATAGTCCGCCTAGAAG)-3′. The sequence of probe #2 is similar to that of probe #1, 5′-amine-$C_6$-(CGCAAGTTAGGTTTTGTCAAGAAAGGGTGTAACGCAACTAAGTCATAGTCCGCCTAGAAG)-(GTGATTGGTCGCGGTGA)-3′. Note that these two sequences possess two identical but constituent blocks, RAFL09 (17 mers) and Bac-alP1 (60 mers), but the orders of the two blocks are reversed. RAFL09 is a fragment of an *Arabidopsis thaliana* gene (Riken Database, accession number AY065271), and Bac-alP1 is a fragment of human beta actin gene (Riken Database, accession number AK223055). Three DNA oligos serve as the targets: (1) cBac-alP1-Cy5 (60 mer), a fully complementary sequence with Bac-alP1 and labeled with Cy5; (2) cRAFL09-Cy3 (17 mer), a fully complementary sequence with RAFL09 and labeled with Cy3; (3) T7-17-Cy3 (17 mer), serving as a negative target with sequence 5′-ATACGACTCACTATAGG-3′-Cy3, which is a complete sequence of plant expression vector pDuExB2 (pDuExD7; NCBI Database, accession number EF565885.1) labeled with Cy3 fluorescence. SP5-Cy5 (60 mer) serves as an immobilization control probe with sequence 5′-GCTGTAACTTATCACACCGTTTCTACAGGTTAGCTAACGAGTGTGCGCAAGTATTAAGTG-amine-3′-C6-Cy5, which is a complete genome of SARS coronavirus strain CV7 (NCBI Database, accession number DQ898174.1) labeled with Cy5 fluorescence. Fig. 1 shows these hybridization configuration designs. All probes and targets were synthesized by ScinoPharm (Tainan, Taiwan) and concentrations were quantified by excluding modified and fluorescent molecules. The chemically coated DNA chips were provided by Phalanx Biotech (Hsinchu, Taiwan) with an amine-reactive surface property. The buffer for preparing probe micro-arrays is a mixture of 20× SSC (Amresco), glycerol (100%, ICN Biomedicals), and $ddH_2O$ (Milli-Q synthesis A10 system). The wash step used a series of concentrations of SSC and SDS buffers, all purchased from Amresco.

#### 2.1.2. Instruments

Micro-arrays were printed with a Cartesian micro-arrayer (PixSys7500, Genomic Solutions, MI, USA). Before the hybridization step, targets were pre-heated to 95 °C on a GeneAmp_PCR machine (9700, Applied Biosystems, CA, USA). Hybridization results were scanned on a GenePix Micro-array scanner (4000B, Molecular Devices, CA, USA). The same provider also gave the software GenePix Pro 4.1 to analyze the scanning images. The hybridization was incubated in a Cocoon hybridization incubator (Bersing Bioscience Tech., Hsinchu, Taiwan) equipped with a plate shaking function. The DNA-chip washes were performed on a Firstek orbital shaker

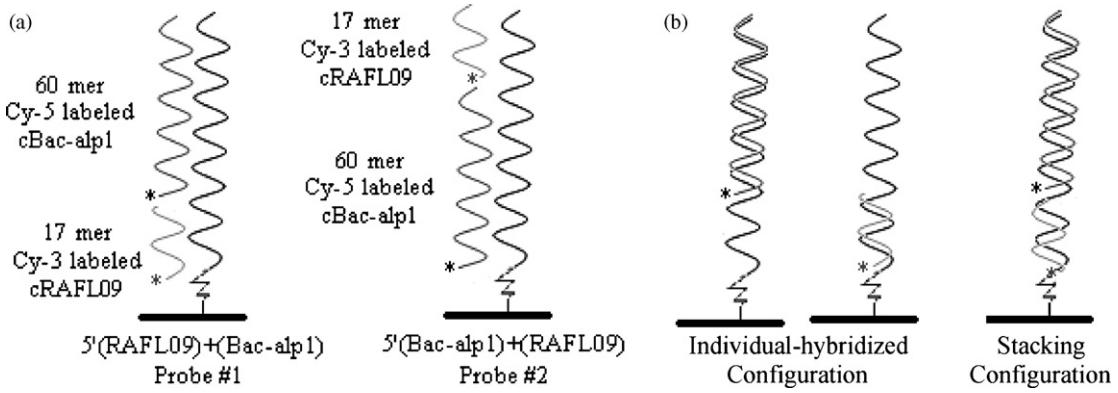


Fig. 1. The experimental design of the DNA probes with their corresponding targets. (a) Two DNA oligos, cBac-alP1 (60 mer) and cRAFL09 (17 mer), labeled with two distinct fluorescent dyes, Cy3 and Cy5, serve as the targets with sequences fully complementary to their shared and immobilized DNA probes in a coaxial stacking configuration. (b) The individual-hybridized and stacking configurations. Note that only two of four individual-hybridized and one of two stacking configurations are shown. The probe molecules could probably also be multi-point attached to the surface due to physisorption or electrostatic interactions with the substrate.

(S101D, Firstek Scientific, Taipei, Taiwan). The TaKaRa™ spaced cover glass for hybridization was purchased from TaKaRa Biotechnology (Shiga, Japan). Wet chips were spun off to dry by a mini spinner (BTCPC100, Bersing Bioscience Tech., Hsinchu, Taiwan).

*2.1.3. Probe micro-arraying and immobilization*

The probes were spotted in micro-arrays with a concentration titration of 150 μM, 100 μM, 50 μM, 10 μM, and 5 μM for the objective probes and 25 μM for the control probe. Ten chips were prepared with two duplicated 6 × 4-array blocks on each chip. The micro-array layout is shown in Fig. 2. The probes were mixed with 20× SSC and 100% glycerol to the fixed final concentrations and loaded onto a 384-hole microtiter plate to perform the micro-arraying, followed by incubation in a humid box at 30 °C for 16–18 h to immobilize the probes on the glass substrates. The spot size was around 600 μm with a vertical spot-to-spot spacing of 1.5 mm and horizontal 1 mm. A wash step was then applied after the immobilization step to remove the free probes by 0.5% SDS for 10 min with shaking at 80 rpm. The slides were then rinsed with $ddH_2O$ and spun to dry.

*2.1.4. DNA hybridization*

In the pre-hybridization treatment, the chips were pre-heated to 50 °C and the 100%-fluorescently labeled target, cRAFL09-Cy3 or cBac-alP1-Cy5, (made by 10 nM+1× hybridization buffer) was prepared in 45 μL. The target was then spread over the chip surface and covered with a TaKaRa™ spaced cover to form a flat reaction slit chamber. Care was taken to avoid creation of trapped air bubbles. The chip was then enclosed in a humid box and incubated at 50 °C for 2 h. The melting temperatures of the target sequences, cRAFL09-Cy3 (17 mer) and cBac-alP1-Cy5 (60 mer), were about 49 °C and 72 °C, respectively. To ensure hybridization efficiency as well as sequence specificity, hybridization temperatures in this study were chosen as 20 °C below melting temperatures of the targets, i.e. around 30 °C and 50 °C, respectively. However, technically, there was no way to hybridize the two targets at two temperatures as they simultaneously existed on the same slide. Therefore, we understood that the hybridization of the 17 mer target at 50 °C was unfavorable, and without the optimal hybridization temperature, Cy3-labeled target would not receive the maximal signal intensity. The fluorescent signals in this study were, however, mainly focused on their relative variation from case to case. Through comparison of various hybridization scenarios at a fixed temperature, it was found that lower intensity readings would not hinder the trend of relative signal variation.

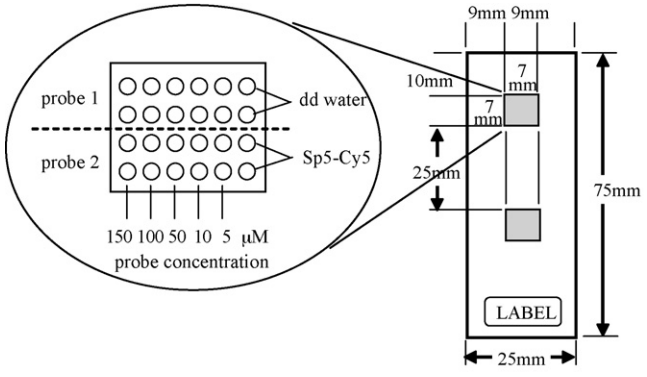


Fig. 2. Layout of the micro-arrays of objective probes. The objective probes were spotted in concentrations of, from left to the right, 150 μM, 100 μM, 50 μM, 10 μM, and 5 μM. The most right column is for the negative (dd water) and positive control (Sp5-Cy5). Two duplicated 6 × 4-array blocks (in shadow) are micro-arrayed on the chip.

In the post-hybridization treatment, the DNA chips were placed in a container and washed in 2× SSC/SDS for 10 min with shaking at 80 rpm. The chips were then washed with 2× SSC in the same condition but without SDS, followed by another wash with 0.2× SSC for 10 min. Finally, the slides were rinsed with $ddH_2O$ and spun to dry.

*2.1.5. Data acquisition and analysis*

The dried chips were scanned by the AXON 4000B scanner with appropriate laser power and PMT settings. The excitation/emission wavelengths of Cy3 were set at 550/570 nm, Cy5 at 649/670, and the scanning resolution at 10 μm. All these parameters were fixed through the study. The raw spot intensities were generated by GenePix Pro version 4.1 software. The analysis process is described as follows. Once the fluorescent images were generated, the software, GenePix Pro 4.1, was executed to analyze the images. It was set to generate a 6 × 4 circle array to cover all micro-arrayed spots to measure the fluorescent signal. The software then automatically saved the analyzed data as excel-format files. The calculation of signal average and standard deviation was then manually undertaken over replicate spots. In this study, there were four replicates located in two zones, with two in each zone. The error bars were produced by taking ± half of their standard deviation.

## 3. Results and discussion

### *3.1. Negative sample test*

To check the non-specific binding of the objective probes, we did a negative sample test by spreading a totally mismatched sample T7-17-Cy3 onto a spotted area and performing hybridization treatments that were identical to the two target sequences to see if any fluorescence was detected. The results showed that the signal detected was less than 0.8% of the lowest reported intensity in Figs. 3–5.

### *3.2. Hybridization of cBac-alP1-Cy5 and cRAFL09-Cy3 with their corresponding probes*

In order to not generate complicated graphs that puzzle the readers, we plot each hybridization condition separately in one figure. We will initially show the individual and then the stacking hybridizing scenarios to step by step demonstrate the readers the steric effect caused by the DNA oligo pre-hybridization on DNA chips.

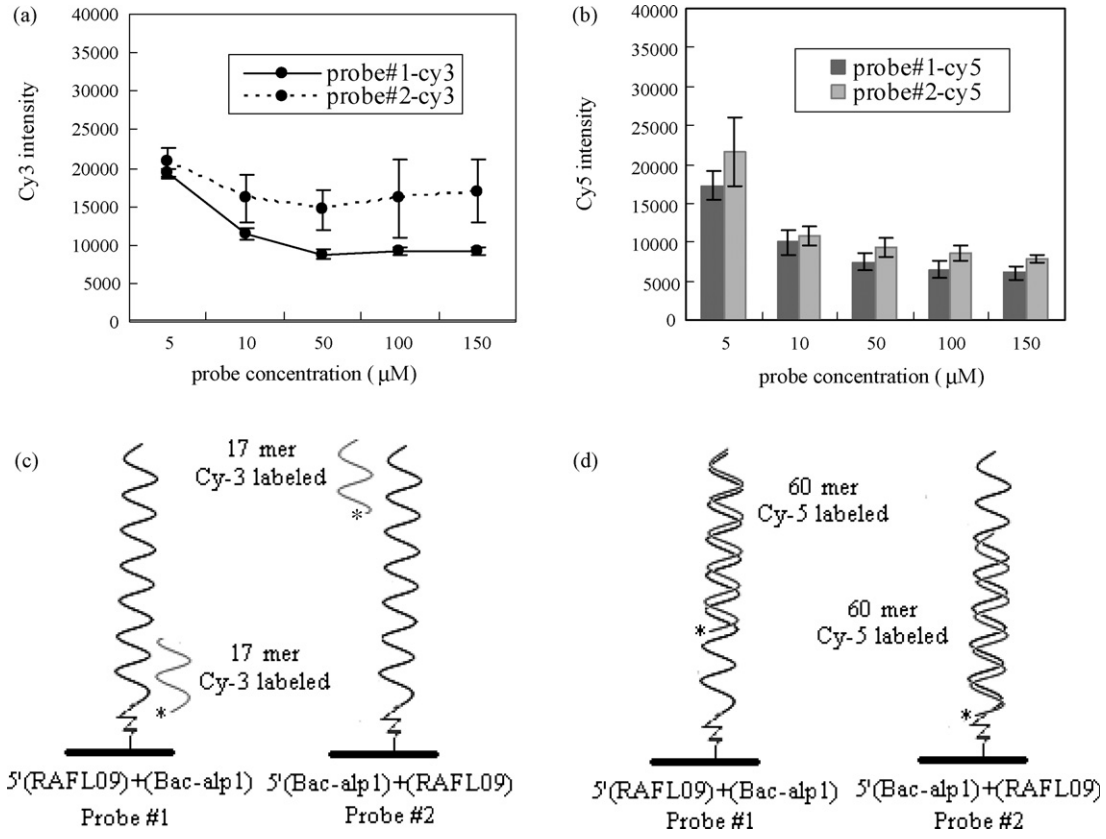


Fig. 3. Individual hybridization of target with two probes. (a and b) Plot of signal intensity versus various probe concentration. Figures presenting in a line style and a bar graph is mainly for facilitating readers to identify fluorescent sources; (c and d) corresponding experimental design of this result.

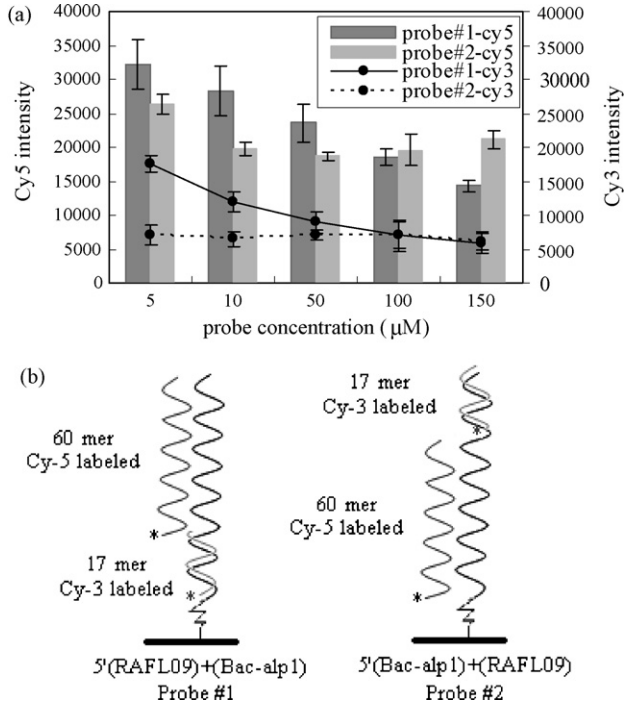


Fig. 4. After consecutive hybridization of probes, first with the 17-mer cRAFL09-Cy3 then the 60-mer Bac-alP1-Cy5 targets. (a) Plot of signal intensity versus probe concentration; (b) corresponding experimental design of this result.

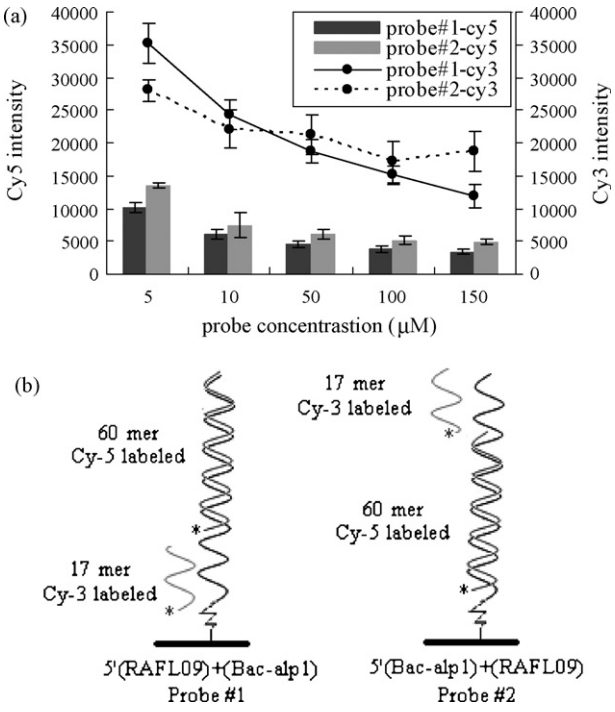


Fig. 5. After consecutive hybridization of probes, first with the 60-mer Bac-alP1-Cy5 then the 17-mer cRAFL09-Cy3 targets. (a) Plot of signal intensity versus probe concentration; (b) corresponding experimental design of this result.

Fig. 3 shows the results for cRAFL09-Cy3 and cBac-alP1-Cy5 individually hybridized with their corresponding probes. The counter-intuitive negative correlation between probe concentration and intensity shown in this figure essentially came from the densely immobilized probes restricting the access of target samples to their complementary binding sites. Comparing these two curves in Fig. 3(a), one may also find that the hindrance effect becomes manifest when the binding sites are located close to the chip surfaces. This site-dependent effect, however, almost disappears for the much larger sized samples labeled with Cy5, as indicated in Fig. 3(b). This is because the whole probe is almost entirely hybridized, so that the location of the binding site on the probe is no longer an important issue. However, further investigation of the effect of probe concentrations on the molecular hindrance should be conducted if a more complete conclusion is desired.

In this study, we are more concerned with the enhancement of hybridization efficiency by the pre-hybridization of DNA sample than the probe-concentration variation. Thus, a second DNA target was added to further demonstrate that issue, as shown in the following section.

### 3.3. cRAFL09-Cy3 followed with cBac-alP1-Cy5 hybridization

Fig. 4 shows the results for the scenario of cRAFL09-Cy3 pre-hybridization on the shared probes followed with cBac-alP1-Cy5. As shown in the figure, with the pre-hybridization of cRAFL09-Cy3, the targeted Cy5 intensities of both hybridized probes dramatically increases up to 87% higher than those of the corresponding hybridization of bare probes shown in Fig. 3(b). This remarkable intensity increase could be attributed to the steric void space created around the bare section of the probe, after the Cy3-labeled sample hybridized, to facilitate the docking of the subsequent Cy5-labeled samples to their binding site in the restricted environment. This demonstration implies that the pre-hybridization of a smaller sized target on the top zone of probes could result in detection-intensity amplification. In addition, from comparison of the two Cy3 curves in Figs. 3(a) and 4(a), one may observe that the Cy3 intensity of probe #2 dramatically drops up to 69% due to the subsequent Cy5-sample hybridization, but intensity of probe #1 has minimal change. The pre-hybridized sample located on the top zone (probe #2) is sacrificed to dissociate from the probe during the subsequent hybridization, however this dissociation is not evident for probe #1. Therefore, the smaller pre-hybridized samples would be easier to dissociate into the free buffer phase above the immobilized probes than into the restricted environment close to the chip surface. Another possibility causing the intensity decrease was the $ddH_2O$ rinse at the end of each wash. $ddH_2O$ is salt free and provides no counter ion; hence, there is no charge shielding for the negatively charged DNA sequences and may cause the DNA duplex to be denaturized.

### 3.4. cBac-alP1-Cy5 followed with cRAFL09-Cy3 hybridization

Fig. 5 shows the results for the case of cBac-alP1-Cy5 pre-hybridization on the shared probes followed with cRAFL09-Cy3 target. This is the reverse scenario of that discussed in the previous section. Similar to the earlier findings, pre-hybridization enhanced the efficiency of the subsequent targeted hybridization. The latter-hybridized Cy3-labeled sample received a tremendous increase in signal intensity up to 82% higher than that of the corresponding individually hybridized case shown in Fig. 3(a). The first-hybridized Cy5-labeled sample was sacrificed up to 66% more than that of the corresponding individual hybridization.

### 3.5. Effect of fluorescent resonance energy transfer

In this study, the targets were 100% fluorescently labeled, such that they might suffer from self-quenching if the dye molecules were in close proximity to one another, i.e. within 10 nm, due to the fluorescence resonance energy transfer (FRET). Thus, the FRET effect was evaluated by comparing the fluorescent intensity generated by 100% with that by 10% or 1% dye-labeled targets. Fig. 6 shows the analysis result for the self-quenching FRET effect. The proportional ratio of Cy5 intensity over various probe concentrations in the figure suggested that there was no self-quenching FRET occurring in

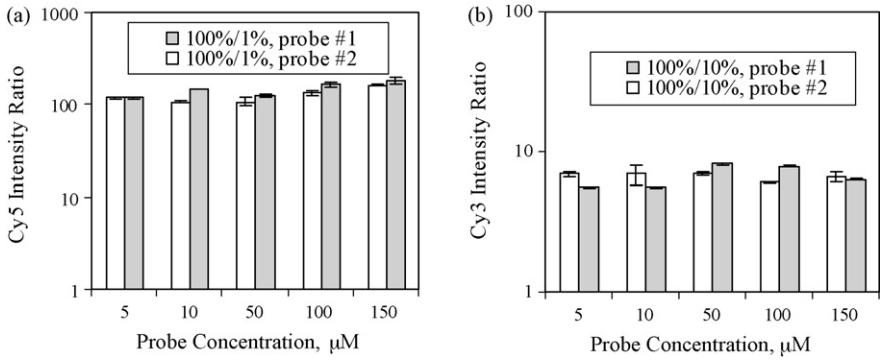


Fig. 6. Investigation of the self-quenching FRET effect over various probe concentrations. (a) Ratio of the Cy5 intensity generated by 100% to that by 1% Cy5-labeled targets. If no self-quenching FRET effect occurred, the ratio should hang around 100. (b) Ratio of the intensity generated by 100% to that by 10% Cy3-labeled targets. If no self-quenching FRET effect occurred, the ratio should hang around 10.

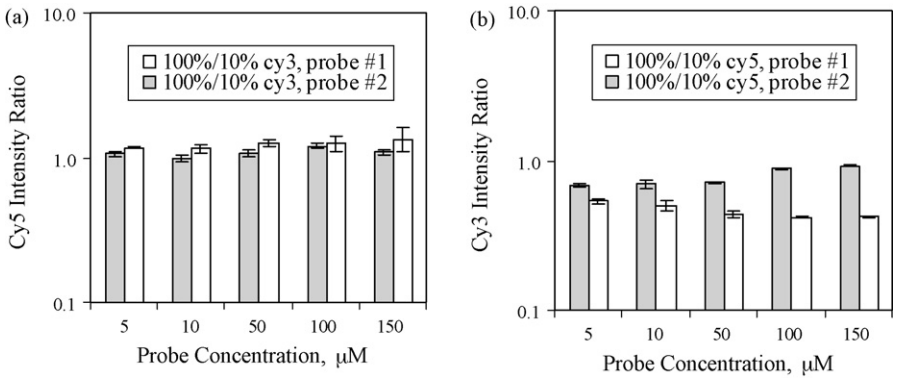


Fig. 7. Investigation of the cross-quenching FRET effect over various probe concentrations. (a) Ratio of the Cy5 intensity quenched by 100% to that by 10% Cy3-labeled targets. (b) Ratio of the Cy3 intensity quenched by 100% to that by 10% Cy5-labeled targets. If no cross-quenching FRET effect occurred, the ratio should both hang around unity.

our original Cy5-fluorescent labeling system. However, the Cy3 dye did suffer a little self-quenching FRET effect, though the quenching extent varied minimally over various probe concentrations. Therefore, our original analysis (Fig. 3(a)) reported a lower intensity reading than reality, but the relative curve trend remained about the same.

Aside from the self-quenching of dyes, our labeling system could also quench the transferred fluorescent energy crossly between Cy3 and Cy5 dyes, which might occur when the two dyes were within 10 nm and were favorably oriented. Particularly in Fig. 4(b), probe #1, the two dyes were separated by a 17 mer DNA, which was around 7–10 nm in length. As a result, a reference study was necessary to ensure that FRET was not present. To perform this study, the single dye-labeled target, cBac-alP1-Cy5, was designed to hybridize onto the probe shared with a target mixture containing 10% cRAFL09-Cy3 and 90% unlabeled cRAFL09. Another experiment was also conducted for the single dye-labeled target, cRAFL09-Cy3, shared probe #1 with 10% cBac-alP1-Cy5 and 90% unlabeled cBac-alP1. By comparing results from this reference study with the original study using both 100% labeled dyes, the effect of FRET can be evaluated. The comparison is shown in Fig. 7.

From Fig. 7(a), the readers can confirm that there was no cross-quenching of Cy5 by Cy3 occurring in our labeling system, since either 100% or 10% Cy3 content made Cy5 reading no difference. However, our labeling system had cross-quenching of Cy3 by Cy5 on both probes, and the quenching effect was more significant on probe #1. This finding could explain why the intensity of Cy3-labeled target decreased after sharing the same probe with Cy5-labeled target in our original study.

## 4. Conclusion

The enhancement of hybridization efficiency by target pre-hybridization on the micro-arrayed-DNA chips was demonstrated by two specially designed DNA probes in two inverse hybridization sequences. The hybridization efficiency was observed to have negative correlation with probe concentration when the oligo target individually hybridizes with its complementary probe. This correlation became manifest when the hybridizing sites were closer to the chip surfaces. Pre-hybridizing the DNA target onto the probe remarkably improved the hybridization efficiency of the subsequent sample hybridized onto the same probe, but the first-hybridized target dissociated and lost detection intensity. Although the two probes in our study did not provide a sufficient data pool to give a global conclusion, the results still implied that an appropriate design of pre-hybridization of probes is able to improve the DNA hybridization efficiency of micro-arrayed gene chips.

## Acknowledgements

Financial support from the Center-of-Excellence Program on Membrane Technology granted by the Ministry of Education and from the National Science Council of the Republic of China under grants NSC 94-2218-E-033-009 (JCW) are gratefully acknowledged.

## References

Deng, P., Y. Lee, and P. Cheng, "Two-Dimensional Micro-Bubble Actuator Array to Enhance the Efficiency of Molecular Beacon Based DNA Micro-Biosensors," *Biosens. Bioelectron.*, **21**, 1443 (2006).

Douglas, C. and J. Ehlting, "Arabidopsis Thaliana Full Genome Longmer Microarrays: A Powerful Gene Discovery Tool for Agriculture and Forestry," *Transgenic Res.*, **14** (5), 551 (2005).

Ezaki, S., S. Haefele, T. Bachmann, and R. Schmidt, "Use of p53 Protein to Increase Efficiency of Hybridization in Microarray Analysis and Detection of Polymorphisms," *European Patent*, DE10, 215, 367 (2003).

Fixe, F., H. Branz, N. Louro, V. Chua, D. Prazeres, and J. Condea, "Immobilization and Hybridization by Single Sub-Millisecond Electric Field Pulses, for Pixel-Addressed DNA Microarrays," *Biosens. Bioelectron.*, **19**, 1591 (2004).

Guo, Z., R. Guilfoyle, A. Thiel, R. Wang, and L. Smith, "Direct Fluorescence Analysis of Genetic Polymorphisms by Hybridization with Oligonucleotide Arrays on Glass Supports," *Nucleic Acids Res.*, **22** (24), 5456 (1994).

Hong, B., V. Sunkara, and J. Park, "NA Microarrays on Nanoscale-Controlled Surface," *Nucleic Acids Res.*, **33** (12), 106/1 (2005).

Koehler, R. and N. Peyret, "Effects of DNA Secondary Structure on Oligonucleotide Probe Binding Efficiency," *Comput. Biol. Chem.*, **29**, 393 (2005).

Luo, Y., A. Chen, and K. Li, "Oligonucleotide Probes with Improved Hybridization Efficiency and Specificity in Detection of Genetic Polymorphisms in Arrays," *European Patent*, WO02, 095, 057 (2002).

Maruyama, A., M. Ueda, W. Kim, and T. Akaike, "Design of Polymer Materials Enhancing Nucleotide Hybridization for Anti-Gene Technology," *Adv. Drug Deliv. Rev.*, **52**, 227 (2001).

McQuain, M., K. Seale, J. Peek, T. Fisher, S. Levy, M. Stremler, and F. Haseltona, "Chaotic Mixer Improves Microarray Hybridization," *Anal. Biochem.*, **325**, 215 (2004).

Rule, G., R. Montagna, and R. Durst, "Characteristics of DNA-Tagged Liposomes Allowing Their Use in Capillary-Migration, Sandwich-Hybridization Assays," *Anal. Biochem.*, **244**, 260 (1997).

Schaack, B., J. Reboud, S. Combe, B. Fouque, F. Berger, S. Boccard, O. Filhol-Cochet, and F. Chatelain, ""DropChip" Cell Array for DNA and siRNA Transfection Combined with Drug Screening," *NanoBiotechnology*, **1** (2), 183 (2005).

Tao, S., H. Gao, F. Cao, X. Ma, and J. Cheng, "Blocking Oligo—A Novel Approach for Improving Chip-based DNA Hybridization Efficiency," *Mol. Cell. Probes*, **17** (4), 197 (2003).

Wang, S. and Q. Cheng, "Microarray Analysis in Drug Discovery and Clinical Applications," *Methods Mol. Biol.*, **316**, 49 (2005).

Wu, J. and J. Prausnitz, "Generalizations for the Potential of Mean Force between Two Isolated Colloidal Particles from Monte Carlo Simulations," *J. Colloid Interface Sci.*, **252**, 326 (2002).

Wu, P., P. Hogrebe, and D. Grainger, "DNA and Protein Microarray Printing on Silicon Nitride Waveguide Surfaces," *Biosens. Bioelectron.*, **21** (7), 1252 (2006).

Zammatteo, N., L. Jeanmart, S. Hamels, S. Courtois, P. Louette, L. Hevesi, and J. Remacle, "Comparison between Different Strategies of Covalent Attachment of DNA to Glass Surfaces to Build DNA Microarrays," *Anal. Biochem.*, **280**, 143 (2000).